Interdomain Interaction and Substrate Coupling Effects on Dimerization and Conformational Stability of Enzyme I of the *Escherichia coli* Phosphoenolpyruvate:Sugar Phosphotransferase System

Mariana N. Dimitrova,[‡] Roman H. Szczepanowski,[‡,§] Sergei B. Ruvinov,[‡,||] Alan Peterkofsky,[⊥,#] and Ann Ginsburg*[,‡]

Section of Protein Chemistry, Laboratory of Biochemistry, and Laboratory of Biochemical Genetics, National Heart, Lung, and Blood Institute, National Institutes of Health, Bethesda, Maryland 20892-8012

Received September 17, 2001

ABSTRACT: The bacterial PEP:sugar phosphotransferase system couples the phosphorylation and translocation of specific sugars across the membrane. The activity of the first protein in this pathway, enzyme I (EI), is regulated by a monomer−dimer equilibrium where a Mg^{2+}-dependent autophosphorylation by PEP requires the dimer. Dimerization constants for dephospho- and phospho-EI and inactive mutants EI(H189E) and EI(H189A) (in which Glu or Ala is substituted for the active site His189) have been measured under a variety of conditions by sedimentation equilibrium at pH 7.5 and 4 and 20 °C. Concurrently, thermal unfolding of these forms of EI has been monitored by differential scanning calorimetry and by changes in the intrinsic tryptophanyl residue fluorescence. Phosphorylated EI and EI(H189E) have 10-fold increased dimerization constants [$\sim 2 \times 10^6$ (M monomer)$^{-1}$] compared to those of dephospho-EI and EI(H189A) at 20 °C. Dimerization is strongly promoted by 1 mM PEP with 2 mM $MgCl_2$ [$K_A' \geq 10^8$ M^{-1} at 4 or 20 °C], as demonstrated with EI(H189A) which cannot undergo autophosphorylation. Together, 1 mM PEP and 2 mM Mg^{2+} also markedly stabilize and couple the unfolding of C- and N-terminal domains of EI(H189A), increasing the transition temperature (T_m) for unfolding the C-terminal domain by ~18 °C and that for the N-terminal domain by ~9 °C to $T_{max} \cong 63$ °C, giving a value of $K_D' \cong 3\ \mu$M PEP at 45 °C. PEP alone also promotes the dimerization of EI(H189A) but only increases T_m ~5 °C for C-terminal domain unfolding without affecting N-terminal domain unfolding, giving an estimated value of $K_D' \cong 0.2$ mM for PEP dissociation in the absence of Mg^{2+} at 45 °C. In contrast, the dimerization constant of phospho-EI at 20 °C is the same in the absence and presence of 5 mM PEP and 2 mM $MgCl_2$. Thus, the separation of substrate binding effects from those of phosphorylation by studies with the inactive EI(H189A) has shown that intracellular concentrations of PEP and Mg^{2+} are important determinants of both the conformational stability and dimerization of dephospho-EI.

The bacterial phosphoenolpyruvate:sugar phosphotransferase system is composed of two cytosolic proteins (enzyme I and HPr) and sugar-specific components (enzymes II). PEP[1] is the phosphoryl donor in a Mg^{2+}-dependent autophosphorylation of enzyme I on the N3 atom of His189. Phosphoenzyme I reversibly transfers its phosphoryl group to the N1 atom of His15 of HPr (*1*). Phosphorylated HPr can donate its phosphoryl group to sugar-specific, membrane-associated enzymes II, which ultimately phosphorylate various sugars for translocation across the membrane (*2*).

Proteolysis and fluorescence studies (*3*−*6*) have shown that enzyme I has a compact amino-terminal domain containing the active site His189 and a less structured, flexible carboxyl-terminal domain that is more susceptible to proteolysis. The amino-terminal domain of *Escherichia coli* enzyme I (EIN) has been cloned and purified by Seok et al. (*7*), who demonstrated, in agreement with the results of LiCalsi et al. (*3*), that EIN can be reversibly phosphorylated in vitro by phospho-HPr but is not autophosphorylated by PEP. EIN is monomeric (*8*, *9*) whereas the C-terminal

* To whom correspondence should be addressed: National Heart, Lung, and Blood Institute, National Institutes of Health, 50 South Drive, Room 2339, Bethesda, MD 20892-8012. Phone: (301) 496-1278. Fax: (301) 480-5492. E-mail: aog@cu.nih.gov.

‡ Section of Protein Chemistry, Laboratory of Biochemistry, National Heart, Lung and Blood Institute.

§ Present address: International Institute of Molecular and Cell Biology, 4 Ks. Trojdena Street, 02-109 Warsaw, Poland.

|| Present address: Center for Scientific Review, Biophysical and Chemical Sciences IRG, National Institutes of Health, 6701 Rockledge Drive, Room 3215-B, Bethesda, MD 20892-7806.

⊥ Laboratory of Biochemical Genetics, National Heart, Lung, and Blood Institute.

Present address: Laboratory of Cell Biology, National Heart, Lung, and Blood Institute, National Institutes of Health, Bethesda, MD 20892-8017.

[1] Abbreviations: PEP, phosphoenolpyruvate; PTS, phosphoenolpyruvate:sugar phosphotransferase system; EI, enzyme I (575 amino acid residues) of the PTS; EIN, amino-terminal domain (residues 1−258 + Arg, containing an introduced C-terminal Arg residue) of EI; dephospho-EI, nonphosphorylated enzyme I; phospho-EI, phosphorylated enzyme I containing phospho-His189; EI(H189E), EI in which the active site His189 has been replaced by Glu; EI(H189A), EI in which the active site His189 has been replaced by Ala; HPr, histidine-containing phosphocarrier protein (~9 kDa); 2-ME, 2-mercaptoethanol; Trp fluorescence, intrinsic tryptophanyl residue fluorescence; DSC, differential scanning calorimetry.

10.1021/bi011801x This article not subject to U.S. Copyright. Published 2002 by the American Chemical Society
Published on Web 12/27/2001

domain contains the contacts necessary for the dimerization of EI (*10*, *11*).

X-ray crystallographic (*12*) and NMR solution (*13*) structures of EIN (residues 1−258 + Arg) show that the nonphosphorylated, active site His189 is buried near the interface between two subdomains: an α/β-domain (residues 1−20 and 148−230) and an α-domain (residues 33−143) consisting of four helices arranged in two hairpins. Upon phosphorylation, His189 rotates toward the surface with only small structural changes detected (*14*). A solution structure for dephospho-EIN complexed to HPr (*15*) shows that HPr binds to the α-subdomain of EIN, and this has been confirmed by Zhu et al. (*10*).

Previously, we have shown that phosphorylation of EIN or EI, or substitution of Glu for His189, significantly destabilizes the amino-terminal domain of enzyme I (*9*, *16*). This observation, together with that of Van Nuland et al. (*17*) on the torsion angle strain introduced into HPr by phosphorylation, led to the proposal that phosphorylation of enzyme I kinetically favors a unidirectional transfer of the phosphoryl group from PEP to enzymes II. The next step, the phosphorylation of the sugar to be translocated across the membrane, is irreversible since the high-energy bond of the phosphoryl groups of EI, HPr, and enzymes II is lost (*2*).

It has been proposed that regulation of the PTS cycle involves a monomer−dimer equilibrium of enzyme I, since only the dimer form of enzyme I is active in the Mg^{2+}-dependent autophosphorylation by PEP (*4*, *18*−*22*). The results reported here, a substrate-promoted increase in the dimerization constant, support this proposal. The availability of the inactive, active site mutant [EI(H189A)] (*16*) has allowed separation of the effects of PEP and Mg^{2+} binding on the dimerization of enzyme I from those of phosphorylation. Moreover, the effects of phosphorylation or the substitution of Ala or Glu for His189 on the monomer−dimer equilibrium of enzyme I in the present study provide evidence for long-range interactions between the N- and C-terminal domains.

EXPERIMENTAL PROCEDURES

Proteins. Mutagenesis of the active site His189 of enzyme I (EI) to Ala or Glu has been described (*16*). Wild-type EI, EI(H189A), and EI(H189E) were expressed and purified from a 2 L culture of either the wild-type strain GI698 (*pts*+) or a Δ*pts* strain transformed with the appropriate expression vectors as described before (*9*). Final yields after concentrating proteins to 2 mL were 60−90 mg. Proteins were homogeneous in SDS−PAGE (*23*) and were stored at −80 °C in the 10 mM Tris-HCl/100 mM NaCl, pH 7.5, buffer used for purification. Proteins were dialyzed overnight at 4 °C against several changes of 10 or 20 mM potassium phosphate ± 100 mM KCl ± 2 mM 2-ME (pH 7.5) buffer using Slide-A-Lyzer cassettes [10000 MW cutoff (Pierce, Rockford, IL)]. Buffers used were either 10 mM potassium phosphate at pH 7.5 and 2 mM 2-ME (buffer A) or 20 mM potassium phosphate, 100 mM KCl, and 2 mM 2-ME, pH 7.5 (buffer B), for ultracentrifugation and fluorescence measurements. For DSC runs, proteins were equilibrated against the same buffers without added thiol (2-ME) or diluted >15-fold into buffers not containing 2-ME. For equilibration of proteins with effectors present, gel filtration through a PD-10 [G25M Sephadex column (Pharmacia, Uppsala, Sweden)] at room temperature was used. Before each measurement, protein concentration was determined spectrophotometrically using the specific absorption coefficient $A_{280nm,1cm} = 0.40$ cm^2/mg determined by Waygood (*24*).

Wild-type enzyme I was dephosphorylated by overnight dialysis at 4 °C against a pH 7.5 buffer containing 10 mM potassium phosphate, 10 mM sodium pyruvate, 1 mM $MgCl_2$, and 2 mM 2-ME, followed by extensive dialysis in the absence of $MgCl_2$ and pyruvate (buffer A). Phosphorylated, wild-type enzyme I was prepared by incubating the dephosphoprotein (15 mg/mL) with 25 mM Tris-HCl, 100 mM NaCl, 5 mM PEP, 2 mM $MgCl_2$, and 2 mM 2-ME, pH 7.5, for 30 min at 25 °C followed by rapid gel filtration of ∼0.25 mL through a PD-10 (G25M Sephadex) column equilibrated with buffer B (± effector ligands) or by overnight dialysis at 4 °C against degassed buffer B at pH 7.5. All chemicals were of the highest purity available, and all solutions were prepared with deionized and filtered water from a Milli-Q Plus system.

Analytical Ultracentrifugation. Beckman Optima Models XL-A and XL-I analytical ultracentrifuges equipped with absorption optics and four-place AN-Ti rotors were used for sedimentation equilibrium experiments at 4 and 20 °C. Cells with carbon-filled six-channel centerpieces (12 mm) and plane quartz windows were used. Generally, the same samples of freshly dialyzed protein were loaded into two cells and run in the two ultracentrifuges at 4.0 and 20.0 °C simultaneously. Protein UV spectra and concentrations from 280 nm absorbances were determined just prior to ultracentrifugation. Proteins were loaded into the right side of each channel: 0.080 or 0.100 mL of ∼0.33−0.40 (inner), 0.56−0.63 (middle), and 0.81−0.94 (outer) mg/mL vs 0.095 or 0.115 mL (0.015 mL more than protein volumes) of reference dialysate buffer in left channels. At the beginning of each run (after temperature equilibration at 3000 rpm), scans at 280 nm (absorbance and intensity) were made in the continuous mode (0.003 cm steps) with three averages at 3000 rpm in order to establish solvent and protein meniscii, plateau absorbances at 280 nm, and bottom radial positions for each channel. Then, rotors were accelerated to 10000 rpm at 20.0 °C and either 10000 or 11000 rpm at 4.0 °C; autoscans at 2 or 4 h intervals were made in 0.001 cm steps (step mode) wth 9−13 averages at either speed for ∼52 h before ending centrifuge runs. Densities of solvents were determined with the Anton-Paar Model DMA-58 densitometer at 20.00 ± 0.01 °C: buffer A, 1.0013 g/mL; buffer B, 1.0079 g/mL. Protein-specific volumes were calculated to be 0.725 mL/g for EI, EI(H189E), and EI(H189A) from the amino acid compositions derived from DNA sequences and the values of Zamyatnin (*25*).

Global, weighted fits of sedimentation equilibrium data obtained at three concentrations of protein to a model of reversible monomer ⇄ dimer association (with fully competent species present) were made using software provided by Allen P. Minton (NIDDK, NIH), which can be downloaded from the Web (http://www.bbri.org/RASMB/rasmb.html). Apparent association constants were floated whereas other parameters such as subunit molecular weight, 1.0 for fraction of competent species, and baselines of zero absorbance were constrained. Trimers and tetramers of enzyme I were not detectible. In all cases, residuals from fits of data to a monomer−dimer equilibrium were randomly distributed

around zero with $<\pm 0.01$ absorbance deviation. In a few cases, some nonequilibrium aggregates were present in protein samples due to extended storage in phosphate buffers at −80 °C or when Hepes buffer ± $MgCl_2$ was used for dialysis, and the data could not be fitted to a model of reversible association.[2] When such nonequilibrium aggregates were detected, either a fresh preparation of the purified protein was made or, in the case of added $MgCl_2$, aggregation was avoided by using gel filtration to equilibrate protein samples (see above).

For conversion of 280 nm absorbance values of apparent dimerization constants ($K_{1,2}^{obs}$) to the true concentration-dependent association constants, K_A' values (expressed per molar concentrations of monomer), it is assumed that the extinction coefficient of the monomer does not change upon dimerization and that the specific absorbance coefficient at 280 nm (A) is 0.40 cm^2/mg (*24*). Thus, $K_{1,2}^{obs} = A_2/A^2 = (2/\epsilon)(K_A')$, where A is the specific absorbance of the monomer and the molar extinction coefficient (ϵ) is for a 1.2 cm path length. Monomer M_r values of 63600 [EI, EI(H189E)] and 63500 [EI(H189A)] are used to calculate ϵ, resulting in the relationship $\log K_A' = 4.184 + \log K_{1,2}^{obs}$. The EI(H189A) mutant in the presence of 1 mM PEP at 20 °C or 1 mM PEP and 2 mM $MgCl_2$ at either 4 or 20 °C is essentially 100% dimer, and the fitted K_A' value (-10^{10} M^{-1}) is greater than the sensitivity of the method. In these cases, $\log K_{1,2}^{obs}$ has been constrained at decreasing values until errors in the global fits of the data significantly increase; since this occurs at values of $K_A' < 10^8$ M^{-1}, K_A' values are reported as $\geq 10^8$ M^{-1}.

Differential Scanning Calorimetry. Most DSC measurements were performed with the VP-DSC calorimeter of Plotnikov et al. (*26*) from MicroCal, Inc. (Northampton, MA), without feedback and with 30−60 min preequilibration at 15 °C before the first scan and between scans. The Nano-1 DSC designed by Privalov et al. (*27*) from Calorimetry Sciences Corp. (Provo, UT) was used for a few experiments with 0.46 mg/mL wild-type enzyme I. DSC instruments were calibrated as previously described (*28*). DSC data were corrected for instrument baselines (determined by buffer vs buffer scans at the same scan rate as used for the protein sample) and normalized for scan rate and protein concentration (2−4 μM enzyme I subunit concentration in experiments with the VP-DSC). For experiments involving PEP, control scans were conducted with PEP added to buffer B vs buffer B in the reference cell, and baselines were found to be the same as buffer−buffer or water−water baselines, indicating that under these conditions hydrolysis of PEP during heating was not significant. Data conversion and analysis were performed using Origin software (MicroCal, Inc.). Excess heat capacity (C_p) was expressed in kcal K^{-1} (mol of monomer)$^{-1}$, where 1.000 cal = 4.184 J.

Fluorescence Spectroscopy. Fluorescence measurements were performed in a SLM Aminco-Bowman Series 2 spectrofluorometer. Measurements were made without polarizers for samples in buffer A (with 4 nm band-pass for excitation at 295 nm and emission at 342 nm) and with polarizers positioned at 54.7° in the emission light beam and 0° for excitation at 295 nm (2 nm band-pass) for samples in buffer B. With polarizers, emission was measured at the intensity maximum for folded EI forms (342 nm) with 8 nm band-pass. The Trp fluorescence of enzyme I was not affected by buffer ionic strength, but the use of polarizers decreased the fluorescence emission intensity ~66%. Temperature was controlled by a programmable Neslab RTE-111 water bath using water-jacketed fluorescence cuvettes (1 mL, 1 cm path length). The sample cuvette temperature was monitored by inserting a microthermocouple (Omega Inc., Stamford, CT) into a jacketed cell containing water, connected in tandem with the sample cuvette. Progress curves for Trp exposure were analyzed by the two-state thermodynamic analysis program of Kirchhoff (*29*). Fluorescence titrations at 20.0 °C of EI(H189A), 0.7 mg/mL, with ≤0.01 mL aliquots of 0.1 M PEP in buffer B (pH 7.5) with 2 mM $MgCl_2$ produced no significant change in Trp fluorescence intensity. Buffer baselines and protein dilutions were made according to Lakowicz (*30*); inner filter effect corrections were not necessary.

RESULTS

Dimerization of Enzyme I. Sedimentation equilibrium experiments with different forms of enzyme I have been conducted under a variety of conditions at 4 and 20 °C using modern ultracentrifugation techniques and absorption optics at 280 nm. The two temperatures have been selected on the basis of previous observations (*31*, *32*) that dimeric enzyme I dissociates at low temperature. Concentration gradients have been analyzed at equilibrium, using a global fit of three concentrations of protein run in a six-channel cell for a reversibly associating monomer−dimer assuming fully competent species present (see Experimental Procedures). Trimeric or tetrameric species are not detected. Representative sedimentation equilibrium data for EI(H189A) after 32 h at 10000 rpm at 4 and 20 °C are shown in Figure 1 (lower panel) for the outer channel together with the global fits of these data to a model of reversible self-association of monomer to dimer (using inner, middle, and outer channels at different protein concentrations). Residuals of the fits of the data sets at each temperature show random distributions around zero with less than ±0.01 absorbance deviation (Figure 1, upper panel). It is apparent that the concentration gradient is steeper at 20 °C than at 4 °C, which reflects the higher apparent association constant for dimerization at the higher temperature. Analyses of these data (Table 1) indeed show that $K_A' = 1.1 \times 10^4$ (M monomer)$^{-1}$ at 4.0 °C and $K_A' = 3.1 \times 10^5$ (M monomer)$^{-1}$ at 20.0 °C, which is a 28-fold increase in the dimerization constant from 4 to 20 °C. Note that dimerization of enzyme I forms occurs at 4 °C, although more weakly than at 20 °C (Table 1).

Dimerization constants (expressed as $\log K_A'$) are given at 4.0 and 20.0 °C in Table 1 for wild-type dephospho- and phospho-EI, EI(H189A), and EI(H189E) at pH 7.5. At low ionic strength, the K_A' value for wild-type dephospho-EI increases 8-fold from 4 to 20 °C, whereas those for EI(H189A) and EI(H189E) increase 36-fold and 3.9-fold from 4 to 20 °C, respectively. Clearly, the additional charge at position 189 adversely affects dimerization in 10 mM

[2] The analysis of sedimentation equilibrium data for reversibly associating macromolecules is very sensitive in detecting nonequilibrium aggregates in solutions of enzyme I. When such aggregates are present, a good fit to a monomer−dimer model for reversible association cannot be made. Since increasing temperature increases the association constant of enzyme I, data obtained at both 4 and 20 °C provide another test for the presence of nonequilibrium aggregates.

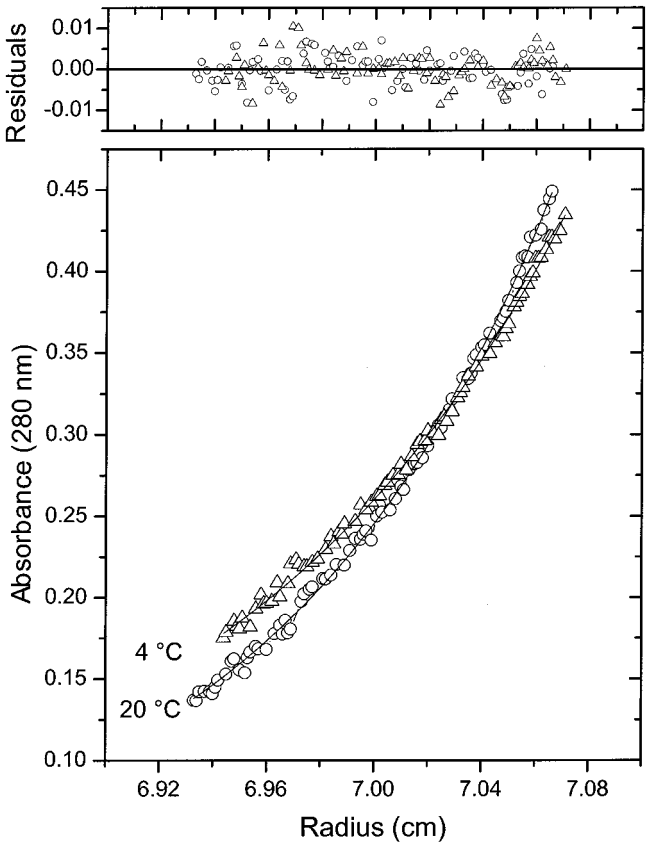

FIGURE 1: Sedimentation equilibrium ultracentrifugation of EI(H189A) at 4 (△) and 20 (○) °C in buffer B. Weighted global fits of the data at three concentrations (0.34, 0.58, and 0.90 mg/mL) for each condition obtained from scans at 280 nm (zero baseline) after 32 h at 10000 rpm are shown in the lower panel for the outer channels by the solid lines. The upper panel shows a plot of the residuals from the global fitting procedure for the data in the figure (≤0.01 absorbance).

potassium phosphate at both 4 and 20 °C. When 100 mM KCl is present, the dimerization constants for wild-type phospho-EI and EI(H189E) increase ~39- and 70-fold from 4 to 20 °C, respectively, whereas that for dephospho-EI increases 3.4-fold and that for EI(H189A) increases 28-fold. Thus, phosphorylation of His189 or the substitution of Glu for His189 increases the dimerization constant at 20 °C from $\sim 2 \times 10^5$ M^{-1} to $\sim 2 \times 10^6$ M^{-1} and also increases the sensitivity to temperature at the higher ionic strength. In contrast, the dimerization of wild-type dephospho-EI is less sensitive to temperature, and that of EI(H189A) is less influenced by increasing ionic strength.

Table 2 presents self-association constants (expressed as log K_A' values) at 4.0 and 20.0 °C for wild-type dephospho-EI and phospho-EI and for EI(H189A) dimerization in the presence of various effectors and 100 mM KCl at pH 7.5. Magnesium ion (2 mM) has little or no effect on increasing the dimerization constant of wild-type EI or EI(H189A) whereas a mixture of 2 mM $MgCl_2$ and 1 mM PEP equilibrated with the inactive EI(H189A) increases the K_A' for dimerization to the extent that essentially only dimer is present at either 4 or 20 °C. In these cases, a value for $K_A' \geq 10^8$ M^{-1} is estimated. In contrast, 5 mM pyruvate has a small adverse effect on the dimerization of dephospho-EI at either 4 or 20 °C. The dimerization constant of phospho-EI was increased ~6-fold at 4 °C (but not significantly affected at 20 °C) by 2 mM $MgCl_2$ and 5 mM PEP (compare Tables 1 and 2). Finally, 1 mM PEP in the absence of Mg^{2+} increases the dimerization constant for EI(H189A) ~140-fold and >332-fold at 4 and 20 °C, respectively. The availability of the inactive EI(H189A) has allowed separation of the effects of binding substrates from those of phosphorylation (see below).

Table 1: Dimerization Constants for Wild-Type Enzyme I and Active Site Mutants [EI(H189A) and EI(H189E)] at pH 7.5 and 4 and 20 °C[a]

enzyme I	buffer	log K_A' (4.0 °C)	log K_A' (20.0 °C)
dephospho-EI(wt)	A	4.192 ± 0.040 (4)	5.108 ± 0.048 (6)
	A (second prepn)	4.029 ± 0.058 (4)	5.240 ± 0.046 (5)
	B	4.763 ± 0.031 (4)	5.305 ± 0.20 (4)
phospho-EI(wt)[b]	B′	4.589 ± 0.033 (6)	6.408 ± 0.189 (7)
	B	4.768 ± 0.044 (7)	6.360 ± 0.075 (6)
EI(H189A)	A	3.977 ± 0.039 (9)	5.533 ± 0.028 (10)
	B	4.036 ± 0.042 (5)	5.490 ± 0.041 (11)
EI(H189E)	A	3.830 ± 0.036 (4)	4.417 ± 0.104 (4)
	B	4.465 ± 0.020 (7)	6.317 ± 0.111 (7)

[a] Dimerization constants are obtained by global fits of sedimentation equilibrium data for a reversibly associating system using data collected at 4 or 20 °C with a six-channel centerpiece for three concentrations of protein (see Experimental Procedures) and are expressed per molar concentration of monomer. The number in parentheses represents the number of global fits of each data set (for one or two separate runs) obtained after reaching equilibrium (≥26 h) to determine the dimerization constant (K_A'); shown are average log K_A' values and the standard deviations from the mean. Buffers used for dialysis are as follows: A, 10 mM potassium phosphate and 2 mM 2-ME, pH 7.5; B, 20 mM potassium phosphate, 100 mM KCl, and 2 mM 2-ME, pH 7.5; B′, same as buffer B but equilibration of samples before ultracentrifugation utilized a PD-10 column (Sephadex G25M, Pharmacia) instead of dialysis. [b] In the case of phospho-EI, buffer A could not be used because the phospho-His189 is considerably more susceptible to hydrolysis in the lower ionic strength buffer than in buffer B.

Table 2: Influence of Effectors on Dimerization Constants of Enzyme I at pH 7.5[a]

enzyme I	effectors	log K_A' (4.0 °C)	log K_A' (20.0 °C)
dephospho-EI (wt)	2 mM $MgCl_2$	4.520 ± 0.032 (7)	5.802 ± 0.026 (7)
	5 mM sodium pyruvate	4.335 ± 0.034 (7)	5.118 ± 0.031 (7)
phospho-EI(wt)	2 mM $MgCl_2$ + 5 mM PEP	5.536 ± 0.025 (4)	6.472 ± 0.110 (4)
EI(H189A)	2 mM $MgCl_2$	4.390 ± 0.014 (5)	5.301 ± 0.082 (6)
	1 mM PEP	6.182 ± 0.242 (8)	≥8 (8)[b]
	2 mM $MgCl_2$ + 1 mM PEP	≥8 (6)[b]	≥8 (6)[b]

[a] Dimerization constants were obtained by global fits of sedimentation equilibrium data as described in Table 1. Proteins were dialyzed against 20 mM potassium phosphate, 100 mM KCl, and 2 mM 2-ME at pH 7.5 and equilibrated on PD-10 columns (Sephadex G25M, Pharmacia) with effectors. The number in parentheses in each case represents the number of the global fits of data obtained at different times (≥26 h) after equilibrium was reached at 11000 rpm (4 °C) or 10000 rpm (20 °C) for determining the standard deviation of the mean for the log of the average association constant K_A' (expressed per molar concentration of monomer) for a reversible monomer−dimer equilibrium. [b] Under these conditions, EI(H189A) was essentially all dimer. Taking into account the detection limits inherent in monitoring protein absorbance at 280 nm, only the lower limits of log K_A' values from global fitting of sedimentation equilibrium data could be determined (see Experimental Procedures).

Thermal Unfolding of Dephospho-EI(wt) and EI(H189A) in the Absence and Presence of Ligands. DSC profiles for thermal unfolding of dephospho-EI(wt) and EI(H189A) after normalization for scan rate and protein concentration and subtraction of the buffer baseline are shown in Figure 2.

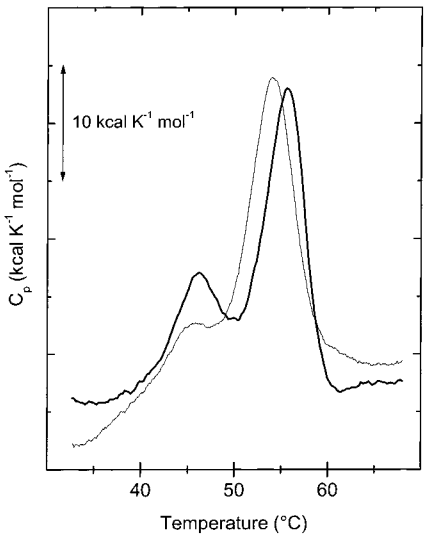

FIGURE 2: First DSC scans obtained at 30 °C/h for dephospho-EI(wt) (0.15 mg/mL, thick line) and EI(H189A) (0.20 mg/mL, thin line) in buffer B without ME (pH 7.5). Each scan is shown after subtraction of the instrument baseline and normalization for concentration and scan rate.

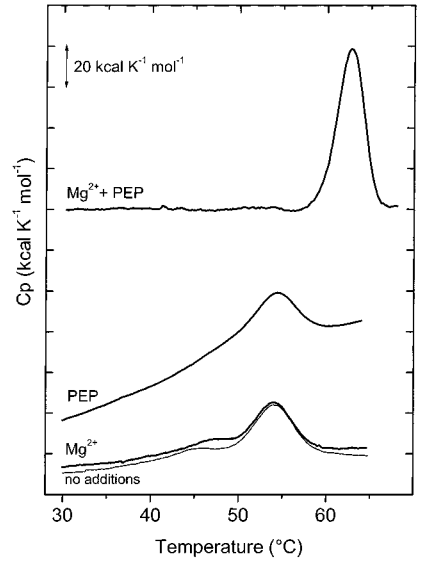

FIGURE 3: DSC scans of EI(H189A) in the absence (thin line) and presence of the effectors 2 mM Mg^{2+}, 1 mM PEP, or 1 mM PEP/2 mM Mg^{2+} (thick lines), respectively, obtained at a scan rate of 60 °C/h in buffer B. Scans are shown after instrument baseline subtraction and normalization for concentration and scan rate. The excess heat capacity of unfolding of EI(H189A) in the presence of 1 mM PEP/2 mM Mg^{2+} is additionally corrected for a protein sigmoidal baseline.

Nonphosphorylated wild-type EI thermally unfolds with two observed endotherms centered at transition temperatures of 46 and 55 °C. The lower T_m value is associated with the unfolding of the C-terminal domain whereas the higher T_m is associated with N-terminal domain unfolding (*3*, *9*). Substitution of Ala for His189 decreases the thermal stability as shown by ~1 °C decreases in maxima of the excess heat capacity for C- and N-terminal domain transitions (Figure 2).

DSC profiles are shown in Figure 3 for EI(H189A) alone and with 2 mM $MgCl_2$, with 1 mM PEP, and with a 1 mM PEP/2 mM $MgCl_2$ mixture in buffer B at pH 7.5. DSC data are from first scans of the protein at a scan rate of 60 °C/h.

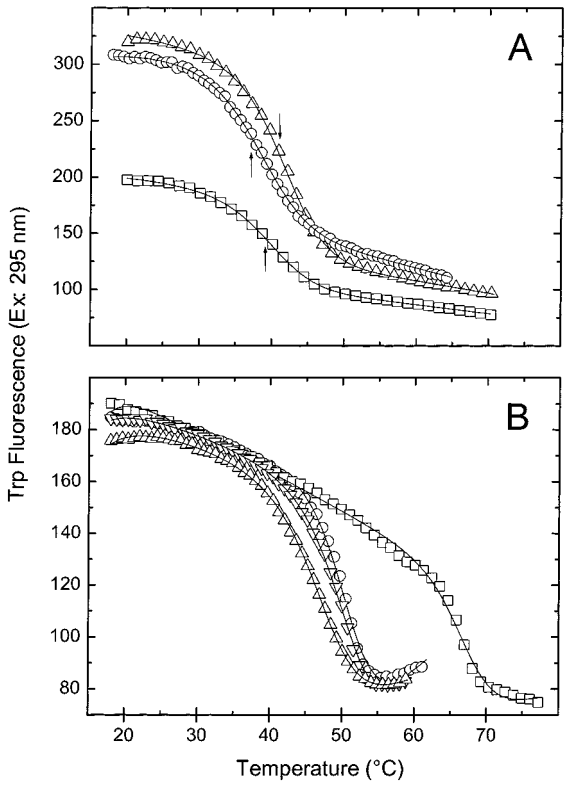

FIGURE 4: Thermally induced changes in Trp residue exposure. Panel A: Trp fluorescence change of dephospho-EI(wt) (○) and the inactive mutants EI(H189A) (△) and EI(H189E) (□) upon heating from 15 to 70 °C in buffer A at a scan rate of 30 °C/h. Protein concentration is 0.15 mg/mL. Panel B: Progress curves for Trp fluorescence changes (with 0.20 mg/mL protein) upon temperature increases for EI(H189A) alone (△), in the presence of 2 mM Mg^{2+} (▽) or 1 mM PEP (○), or with a mixture of 1 mM PEP and 2 mM Mg^{2+} (□) in buffer B at a scan rate of 60 °C/h. The fit of each data set to a two-state model of unfolding is shown by a solid line, and the positions of the transition temperatures for fitted curves are marked by arrows in panel A; see Table 3 for parameters of the fits to a model of two-state unfolding for the data given in panel B.

The addition of 2 mM Mg^{2+} gives a 2 °C stabilization of the C-terminal domain without changing the unfolding transition temperature of the N-terminal domain. Similarly, the presence of 1 mM PEP in the absence of Mg^{2+} stabilizes the C-terminal domain, increasing T_m ~5 °C without influencing the unfolding of the N-terminal domain. In contrast, the presence of both Mg^{2+} and PEP with EI(H189A) stabilizes and couples the unfolding of both the C- and N-terminal domains, yielding a single endotherm with a midpoint transition temperature of ~63 °C.

Thermally Induced Changes in the Trp Fluorescence of Enzyme I and EI Active Site Mutants in the Absence and Presence of Active Site Ligands. The two Trp residues, at positions 357 and 498, of EI are both located in the flexible C-terminal domain of the protein. Measurements of changes in Trp fluorescence of the protein therefore reflect conformational changes predominantly occurring in the C-terminal domain. Thermally induced changes in Trp residue exposure for wild-type, dephospho-EI, EI(H189A), and EI(H189E) during heating from 15 to 70 °C in buffer A are illustrated in Figure 4 A. Progress curves of the Trp fluorescence changes as a function of increasing temperature are shown by the open symbols, and the fit of each data set to a two-state model of unfolding is depicted by a solid line. Arrows

mark the positions of transition temperatures for fitted curves. For all three proteins, the data are fitted well to a two-state model of unfolding which yields T_m values of 36.8, 41.1, and 38.8 °C and ΔH values of 47, 61, and 54 kcal mol^{-1}, respectively, for dephospho-EI(wt), EI(H189A), and EI(H189E). For the data in Figure 4A, protein samples are 0.15 mg/mL in 10 mM potassium phosphate (pH 7.5) containing 2 mM ME. Unfolding transitions are reversible under these conditions; i.e., the same transition is observed during a second heating after cooling to 15 °C for 1 h (*9*). Under the conditions of Figure 4 A, >85% of the enzyme I proteins are monomeric (Table 1). The initial fluorescence of EI(H189E) and the amplitude of the Trp fluorescence change during thermal unfolding are approximately two-thirds and one-half, respectively, of those of either EI(wt) or EI(H189A). This may be related to a different conformation of EI(H189E) (*16*) and/or charge transfer from the substituted glutamate residue at position 189 to Trp residues in the C-terminal domain.

Panel B of Figure 4 illustrates the influence of 2 mM Mg^{2+}, 1 mM PEP, and a PEP/Mg^{2+} mixture on the unfolding of the C-terminal domain of EI(H189A) in high ionic strength buffer (buffer B) upon heating from 15 to ≤80 °C. As in Figure 4A, fits of the data to a two-state unfolding model are shown by the solid lines. Posttransitional baselines are less reliable than at low ionic strength due to aggregation that occurs in buffer B at high temperature, and scans are not repeatable after cooling from high temperatures. The presence of either 2 mM Mg^{2+} or 1 mM PEP leads to ∼4 °C stabilization of the C-terminal of EI(H189A) when scanned at a rate of 60 °C/h. The addition of a mixture of $MgCl_2$ and PEP at the same concentrations markedly stabilizes the C-terminal domain, increasing the transition temperature by >16 °C. The parameters from two-state analysis of intrinsic Trp fluorescence changes of EI(H189A) with and without effectors during thermal unfolding approximately agree with those from deconvolution of DSC data for C-terminal domain unfolding (Table 3).

The initial Trp fluorescence of EI(H189A) at 20 °C in the absence and presence of the mixture of Mg^{2+} and PEP is approximately the same even though the combination of these effectors strongly promotes dimerization (Table 2). In addition, titrations of EI(H189A) with PEP in the presence of 2 mM $MgCl_2$ produce no significant change in Trp fluoresence (data not shown). Initial Trp fluorescence values of EI(H189A) differ in panels A and B of Figure 4 because in panel B (and not in panel A) polarizers have been used (see Experimental Procedures).

Analysis of DSC Data. Parameters from fits of DSC data to either a model of two independent, two-state transitions or to a sequential model (in the presence of PEP and/or Mg^{2+}) during thermal unfolding are summarized in Table 3. Except in the case of EI(H189A) in the presence of PEP and Mg^{2+}, coupling of domain unfolding is sufficiently weak that DSC data are fit well by a random model of unfolding without detectable unfolding intermediates populated other than those attributed to C-and N-terminal domain random unfolding. Previous evidence of energetic coupling between N- and C-terminal domains is based on the observations that the isolated N-terminal domain is 3 °C more stable than that in the intact, full-length enzyme I (*3*, *9*). Thus, the C-terminal domain has a destabilizing effect on the N-terminal domain,

Table 3: Summary of Thermodynamic Parameters for Thermal Unfolding of Dephospho-EI(wt) and EI(H189A) in the Absence and Presence of Effectors[a]

protein, mg/mL	effector(s) present[b]	T_m^1 (°C)	T_m^2 (°C)	ΔH_1 (kcal/mol)	ΔH_2 (kcal/mol)	scan rate (°C/h)
EI(wt), 0.24	− (R)	46.9	56.1	98 (88)	153 (135)	60
Fl		45.0		75		60
EI(wt), 0.15	− (R)	46.4	55.4	74 (103)	127 (175)	30
Fl		43.0		77		30
EI(wt), 0.46	− (R)	46.2	55.1	77 (103)	163 (158)	30[c]
EI(wt), 0.20	pyruvate (R)	46.6	56.3	65 (107)	155 (155)	60
EI(wt), 0.16	pyruvate (R)	46.0	55.5	83 (90)	157 (168)	30
EI(H189A), 0.20	− (R)	45.2	54.0	48 (100)	145 (147)	60
Fl		46.8		63		60
EI(H189A), 0.20	− (R)	45.4	54.4	45 (99)	140 (150)	30
EI(H189A), 0.16	− (R)	43.4	53.6	38 (130)	139 (156)	30[d]
Fl		41.8		67		30[d]
EI(H189A), 0.21	Mg^{2+} (R)	47.0	54.0	46	140	60
Fl	Mg^{2+}	50.6		86		60
EI(H189A), 0.20	Mg^{2+} (R)	47.4	54.6	50	147	30
Fl	Mg^{2+}	49.0		70		30
EI(H189A), 0.26	PEP (R)	49.5	54.4	65	131	60
Fl	PEP	50.8		75		60
EI(H189A), 0.26	PEP (R)	49.9	54.6	111	130	30
EI(H189A), 0.22	Mg^{2+}/PEP (D)	62.8	62.3	130	160	60
Fl	Mg^{2+}/PEP	65.8		96		60
Fl	Mg^{2+}/PEP	64.6		94		30

[a] Thermodynamic parameters (except those designated Fl) are obtained from deconvolutions of DSC data assuming a model of either two independent, two-state transitions (R = random) or sequential transitions (D = dependent). Standard errors in T_m are ±0.2 °C and ±10% in ΔH values. The numbers in parentheses show calculated van't Hoff enthalpies for two-state unfolding of each domain in the absence of effectors obtained from deconvolutions of DSC data. Entries designated Fl are from two-state analysis of intrinsic Trp fluorescence changes as a function of increasing temperature for C-terminal domain unfolding in the presence of 2 mM 2-ME. Proteins have been equilibrated with 20 mM potassium phosphate and 100 mM KCl, pH 7.5, buffer in the absence and presence of effectors (see Experimental Procedures) except as indicated otherwise. [b] Concentrations of effectors are 5 mM sodium pyruvate, 2 mM $MgCl_2$, and 1 mM PEP when present. [c] DSC data are from the Nano-1 DSC, whereas all other values in the table are from experiments with the VP-DSC. [d] DSC experiments with EI(H189A) in 10 mM potassium phosphate (pH 7.5).

and perhaps this is a factor in giving good fits of DSC data for intact, wild-type enzyme I to a model of two independent, two-state transitions. In any case, fits of fluorescence data to a model of two-state unfolding of the C-terminal domain (Figure 4) give parameters that are in fair agreement with those obtained from deconvolutions of DSC data obtained at 30 or 60 °C/h scan rates (Table 3). The effectors Mg^{2+} or PEP alone stabilize the C-terminal domain of EI(H189A) by ∼2 and 5 °C, respectively, without significantly influencing the unfolding parameters for N-terminal domain unfolding. Clearly, these ligands bind to the C-terminal domain. However, when a mixture of 2 mM Mg^{2+} and 1 mM PEP is present, both the C- and N-terminal domains are stabilized by ∼18 and 9 °C, respectively (Table 3). Thus, a mixture of Mg^{2+} and PEP couples the unfolding of both the C- and N-terminal domains (Figure 3) whereas either ligand alone at the same concentration only exerts a stabilizing effect on the C-terminal domain.

Stabilizing effects of ligands on the C-terminal domain of enzyme I occur through the binding energy (*33*, *34*). Thus, the effect of a ligand (L) on the transition temperature for a two-state unfolding of a macromolecule (with $T_c \geq T_0$) is directly related to the affinity constant for the ligand (*33*, *34*). Assuming that the ligand binds to a single site of each subunit and does not bind to unfolded C-terminal domains of EI(H189A), eq 17 of Brandts (*33*) can be applied:

$$\ln(1 + K_L[L]) = (\Delta H_0/R)(1/T_0 - 1/T_c) - \Delta C_p/R[\ln(T_0/T_c) + T_c/T_0 - 1] \quad (1)$$

where T_0 and T_c are transition midpoints in the absence and presence of ligand L, respectively; [L] is the free concentration of ligand; ΔH_0 is the van't Hoff enthalpy change for two-state unfolding of the C-terminal domain at midpoint T_0 in the absence of ligand; and ΔC_p is the heat capacity change for unfolding, which in this case is assumed to be 3300 cal K^{-1} mol^{-1} or the same as that measured for EIN in buffer B (*16*). Since the protein had been equilibrated against buffer B containing the indicated concentration of ligand before DSC experiments and the concentration of ligand is >240-fold that of the protein, the free concentration of the ligand is known.

Using eq 1 (*33*) and the above assumptions, estimated values of $K_D' = 3.0 \pm 0.2$ μM for PEP dissociation from complexed EI(H189A) at 45 °C are calculated from data obtained at 60 and 30 °C/h scan rates for C-terminal domain unfolding in the presence of both Mg^{2+} and PEP (Table 3). Again, using the T_m and ΔH_0 values at 30 and 60 °C/h scan rates in Table 3 and assuming the above ΔC_p value, eq 1 has been used to calculate K_D' values of 0.16 ± 0.01 mM for PEP in the absence of Mg^{2+} at 45 °C. The same calculation for EI(H189A) in the presence of 2 mM Mg^{2+} requires more information than is presently available, since divalent cations can bind to more than one site of both folded and unfolded forms of proteins (*35*). Nevertheless, it is apparent that there is a large synergistic effect between the binding of PEP and Mg^{2+} to EI(H189A). A K_m value of 0.53 mM Mg^{2+} for the autophosphorylation of EI by PEP at 25 °C has been reported by Weigel et al. (*36*).

It is possible that pyruvate binds to both folded and unfolded EI since 5 mM pyruvate has no apparent effect on the transition temperature for C-terminal domain unfolding (Table 3). It is also possible that the weak binding of pyruvate to enzyme I destabilizes the C-terminal domain, as manifested by a lower dimerization constant of dephospho-EI in the presence of 5 mM pyruvate at 20 °C (Table 2).

DISCUSSION

Enzyme I of the PEP:sugar phosphotransferase system catalyzes the first reaction in a cascade of events that leads to translocation of sugars across the membrane. It has been firmly established (*4*, *18*−*22*) that the initial step in the PTS, the Mg^{2+}-dependent autophosphorylation of enzyme I by PEP, requires the self-associated dimer. The cloned N-terminal domain (EIN) is monomeric (*8*, *9*) whereas the highly conserved C-terminal domain contains the regulatory protein−protein interactions for dimerization of enzyme I, and in fact, the cloned C-terminal domain dimerizes with high affinity, $\geq 10^8$ M^{-1} (*10*, *11*). Phosphorylation or substitution of Glu for His189 produces a destabilizing conformational change in the N-terminal domain (*9*, *16*) that is shown here to cause an approximate 10-fold *increase* in the dimerization constant at 20 °C: from $\sim 2 \times 10^5$ M^{-1} for dephospho-EI or EI(H189A) to $\sim 2 \times 10^6$ M^{-1} for phospho-EI or EI(H189E); see Table 1. That is, long-range interactions between the N- and C-terminal domains occur. These results are consistent with previous kinetic studies (*20*, *37*) that demonstrate that Mg^{2+} and PEP shift the monomer−dimer equilibrium of enzyme I to the enzymatically active dimer by decreasing the dissociation rate of the phosphorylated dimer. It has been shown here that Mg^{2+} and PEP do not significantly affect the monomer−dimer equilibrium of already phosphorylated enzyme I at 20 °C (see Table 2).

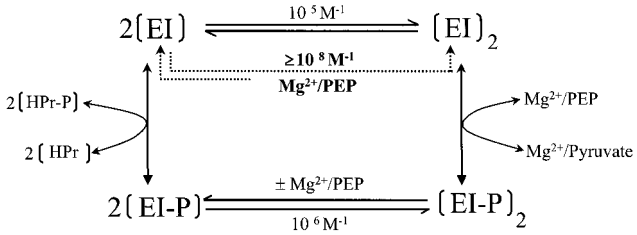

FIGURE 5: Scheme of reversible monomer ⇌ dimer equilibria for enzyme I at pH 7.5 and 20 °C. The approximate magnitudes of association constants from sedimentation equilibrium studies in the absence and presence of PEP and Mg^{2+} are shown. The equilibria shown on top are for the dimerization of wild-type, dephospho-EI and below that is the postulated dimerization of EI promoted by binding PEP and Mg^{2+} (dotted line) before phosphorylation occurs [based on results obtained with EI(H189A) in the presence of 2 mM $MgCl_2$ and 1 mM PEP]. The dephospho-EI dimer catalyzes a Mg^{2+}-dependent autophosphorylation by PEP, and, once phosphorylated (EI-P), the reversible dimer ⇌ monomer equilibrium is shown at the bottom. Pyruvate at relatively high concentrations in the presence of Mg^{2+} reverses autophosphoryation of EI. Phosphotransfer to the histidine-containing phosphocarrier protein (HPr) may not require monomeric phospho-EI (see text).

By studying the effects of Mg^{2+} and/or PEP on the monomer−dimer equilibrium and the conformational stability of the inactive, active site mutant EI(H189A), we have been able to separate the effects of binding these ligands from phosphorylation effects. This is illustrated in the scheme of Figure 5. In sedimentation equilibrium experiments with wild-type dephospho-EI or EI(H189A), a dimerization constant at 20 °C of $\sim 10^5$ (M monomer)$^{-1}$ has been measured. However, the dimerization constant for EI(H189A) in the presence of 2 mM Mg^{2+} and 1 mM PEP is increased at least 3 orders of magnitude to $\geq 10^8$ M^{-1} by the binding of these effectors (Tables 1 and 2). Once phosphorylated, enzyme I [or EI(H189E)] has a dimerization constant at 20 °C of $\sim 2 \times 10^6$ M^{-1} (Table 1), which is essentially the same in the absence and presence of Mg^{2+} and PEP (Table 2; Figure 5).

As recently discussed by Brokx et al. (*11*), it is not certain whether phospho-enzyme I must be monomeric for phosphotransfer to HPr as originally proposed (*1*). The affinity constant for binding of HPr to EIN and EI [or to EI(H189E)] is approximately the same with $K_A' \cong (1-3) \times 10^5$ M^{-1} (*8*, *16*), and moreover, phosphorylation favors the dimer. Nevertheless, phosphotransfer from phospho-EI to HPr will promote the formation of monomeric EI due to the difference in the dimerization constants between phospho-EI and dephospho-EI (Figure 5). However, the presence of ~ 2 mM Mg^{2+} and ≥ 0.3 mM PEP promotes full dimerization of dephospho-EI. Thus, intracellular PEP (*38*) and Mg^{2+}

concentrations are the major determinants of enzyme I activity in the first step of the PTS, i.e., the Mg^{2+}-dependent autophosphorylation of enzyme I by PEP.

In addition to increasing the dimerization constant for EI(H189A) by at least 3 orders of magnitude, the binding of PEP in the presence of 2 mM Mg^{2+} and 1 mM PEP markedly stabilizes and couples the thermal unfolding of both C- and N-terminal domains, as demonstrated by DSC (Figure 3). The transition temperature for unfolding the C-terminal domain [to which PEP binds (*11*, *39*)] increases ~18 °C and that for N-terminal domain unfolding increases ~9 °C to $T_{max} \cong 63$ °C in the presence of 2 mM Mg^{2+} and 1 mM PEP. From the increase in the observed T_m value for C-domain unfolding produced by 1 mM PEP amd 2 mM $MgCl_2$ and assuming that PEP only binds to the folded form, eq 1 gives a K_D' value of 3.0 ± 0.2 μM for dissociation of PEP from the C-domain in the presence of 2 mM Mg^{2+} at 45 °C. This value is much lower than the range of reported K_m values for PEP, 0.2−0.4 mM (*38*), using a coupled assay with lactate dehydrogenase at 25 °C.

Although 1 mM PEP in the absence of Mg^{2+} does not couple the unfolding of the C- and N-terminal domains of EI(H189A), the C-domain is stabilized ~5 °C by the presence of 1 mM PEP alone (Table 3). This result gives an estimated K_D' value of ~0.16 mM for PEP in the absence of Mg^{2+} at 45 °C. Thus, the binding of PEP and Mg^{2+} is synergistic. The binding of PEP to EI(H189A) in the absence of Mg^{2+} also promotes dimerization at 20 °C (Table 2), but clearly Mg^{2+} is required for domain coupling and increasing the affinity of the enzyme for PEP. Certainly, the autophosphorylation of enzyme I by PEP is dependent on the presence of Mg^{2+} (*1*), and this divalent cation may play an important role in orienting the phosphoryl group during transfer in addition to stabilizing the enzymatically active protein conformation.

Recently, Rohwer et al. (*38*) have measured the in vivo concentrations of PEP for resting cells and those in which the translocation of sugars is operating efficiently. Concentrations of PEP were 2.8 mM and ~0.06−0.30 mM for the former and latter conditions. Clearly, the availability of PEP and Mg^{2+} regulates the initiation of the PTS cycle by promoting the dimerization of enzyme I.

ACKNOWLEDGMENT

The authors thank Dr. Grzegorz Piszczek for help in the analysis of DSC data and in various aspects of the manuscript preparation.

REFERENCES

1. Meadow, N. D., Fox, D. K., and Roseman, S. (1990) *Annu. Rev. Biochem. 59*, 497−542.
2. Postma, P. W., Lengeler, J. W., and Jacobson, G. R. (1996) in *Escherichia coli and Salmonella*: *Cellular and Molecular Biology* (Neidhardt, F. C., Ed.) pp 1149−1174, American Society for Microbiology Press, Washington, DC.
3. LiCalsi, C., Crocenzi, T. S., Freire, E., and Roseman, S. (1991) *J. Biol. Chem. 266*, 19519−19527.
4. Chauvin, F., Brand, L., and Roseman, S. (1996) *Res. Microbiol. 147*, 471−479.
5. Han, M. K., Roseman, S., and Brand, L. (1990) *J. Biol. Chem. 265*, 1985−1995.
6. Lee, B. R., Lecchi, P., Pannell, L., Jaffe, H., and Peterkofsky, A. (1994) *Arch. Biochem. Biophys. 312*, 121−124.
7. Seok, Y.-J., Lee, B. R., Zhu, P.-P., and Peterkofsky, A. (1996) *Proc. Natl. Acad. Sci. U.S.A. 93*, 347−351.
8. Chauvin, F., Fomenkov, A., Johnson, C. R., and Roseman, S. (1996) *Proc. Natl. Acad. Sci. U.S.A. 93*, 7028−7031.
9. Nosworthy, N. J., Peterkofsky, A., König, S., Seok, Y.-J., Szczepanowski, R. H., and Ginsburg, A. (1998) *Biochemistry 37*, 6718−6726.
10. Zhu, P.-P., Szczepanowski, R. H., Nosworthy, N. J., Ginsburg, A., and Peterkofsky, A. (1999) *Biochemistry 38*, 15470−15479.
11. Brokx, S. J., Talbot, J., Georges, F., and Waygood, E. B. (2000) *Biochemistry 39*, 3624−3635.
12. Liao, D.-I., Silverton, E., Seok, Y.-J., Lee, B. R., Peterkofsky, A., and Davies, D. R (1996) *Structure 4*, 861−872.
13. Garrett, D. S., Seok, Y.-J., Liao, D.-I., Peterkofsky, A., Gronenborn, A. M., and Clore, G. M. (1997) *Biochemistry 36*, 2517−2530.
14. Garrett, D. S., Seok, Y.-J., Peterkofsky, A., Clore, G. M., and Gonenborn, A. M. (1998) *Protein Sci. 7*, 789−793.
15. Garrett, D. S., Seok, Y.-J., Peterkofsky, A., Gronenborn, A. M., and Clore, G. M. (1999) *Nat. Struct. Biol. 6*, 166−173.
16. Ginsburg, A., Szczepanowski, R. H., Ruvinov, S. B., Nosworthy, N. J., Sondej, M., Umland, T. C., and Peterkofsky, A. (2000) *Protein Sci. 9*, 1085−1094.
17. Van Nuland, N. A. J., Wiersma, J. A., Van der Spoel, D., De Groot, B. L., Scheek, R. M., and Robillard, G. T. (1996) *Protein Sci. 5*, 442−446.
18. Waygood, E. B., Meadow, N. D., and Roseman, S. (1979) *Anal. Biochem. 95*, 293−304.
19. Saier, M. H., Schmidt, M. R., and Lin, P. (1980) *J. Biol. Chem. 255*, 8579−8584.
20. Misset, O., Brouwer, M., and Robillard, G. T. (1980) *Biochemistry 19*, 883−890.
21. Kukuruzinska, M. A., Turner, B. W., Ackers, G. K., and Roseman, S. (1984) *J. Biol. Chem. 259*, 11679−11681.
22. Seok, Y.-J., Zhu, P.-P., Koo, B.-M., and Peterkofsky, A. (1998) *Biochem. Biophys. Res. Commun. 250*, 381−384.
23. Laemmli, U. K. (1970) *Nature (London) 227*, 680−685.
24. Waygood, E. B. (1986) *Biochemistry 25*, 4085−4090.
25. Zamyatnin, A. (1984) *Annu. Rev. Biophys. Bioeng. 13*, 145−165.
26. Plotnikov, V. V., Brandts, J. M., Lin, L.-N., and Brandts, J. F. (1997) *Anal. Biochem. 250*, 237−244.
27. Privalov, G., Kavina, V., Freire, E., and Privalov, P. L. (1995) *Anal. Biochem. 232*, 79−85.
28. Ginsburg, A., and Zolkiewski, M. (1991) *Biochemistry 30*, 9421−9429.
29. Kirchhoff, W. H. (1993) *NIST Technical Note 1401*: EXAM, 110 pages (CODEN: NTNOEF) U.S. Government Printing Office, Washington, DC.
30. Lakowicz, J. R. (1999) in *Principles of Fluorescence Spectroscopy*, 2nd ed., Kluwer Academic/Plenum Publishers, New York.
31. Robillard, G. T., Dooijewaard, G., and Lolkema, J. (1979) *Biochemistry 18*, 2984−2989.
32. Waygood, E. B., and Steeves, T. (1980) *Can. J. Biochem. 58*, 40−48.
33. Brandts, J. F., Hu, C. Q., Lin, L.-N., and Mas, M. T. (1989) *Biochemistry 28*, 8588−8596.
34. Becktel, W. J., and Schellman, J. A. (1987) *Biopolymers 26*, 1859−1877.
35. Shrake, A., Fisher, M. T., McFarland, P. J., and Ginsburg, A. (1989) *Biochemistry 28*, 6281−6294.
36. Weigel, N., Waygood, E. B., Kukuruzinska, M. A., Nakazawa, A., and Roseman, S. (1982) *J. Biol. Chem. 257*, 14461−14469.
37. Hübner, G., König, S., Koch, M. H. J., and Hengstenberg, W. (1995) *Biochemistry 34*, 15700−15703.
38. Rohwer, J. M., Meadow, N. D., Roseman, S., Westerhoff, H. V., and Postma, P. W. (2000) *J. Biol. Chem. 275*, 34909−34921.
39. Seok, Y.-J., Lee, B. R., Gazdar, C., Svenson, I., Yadla, N., and Peterkofsky, A. (1996) *Biochemistry 35*, 236−242.

BI011801X